ACS Sustainable Chemistry & Engineering

Research Article

pubs.acs.org/journal/ascecg

Facile Preparation of Lignosulfonate–Graphene Oxide–Polyaniline Ternary Nanocomposite as an Effective Adsorbent for Pb(II) Ions

Jun Yang, Jun-Xiong Wu, Qiu-Feng Lü,* and Ting-Ting Lin

College of Materials Science and Engineering, Fuzhou University, 2 Xueyuan Road, Fuzhou 350116, People's Republic of China

ABSTRACT: A new nanocomposite, lignosulfonate–graphene oxide–polyaniline (LS-GO-PANI), was prepared from aniline via an *in situ* polymerization in the presence of lignosulfonate and graphene oxide. The morphology and structure of the LS-GO-PANI ternary nanocomposite were characterized by FE-SEM, TEM, FTIR, and UV–vis spectroscopy. Furthermore, the adsorption property of Pb(II) ions onto the nanocomposite was studied. The effects of adsorption time, initial pH value, adsorbent concentration, and initial adsorbate concentration on the adsorption of Pb(II) ions in aqueous solution were investigated by batch experiments. The LS-GO-PANI ternary nanocomposite showed an adsorption capacity as high as 216.4 mg g^{-1} for Pb(II) ions at 30 °C. Moreover, the adsorption kinetic and equilibrium data were described well with the pseudo-second-order and Langmuir isotherm models for the Pb(II) ions adsorption process. The results showed that the LS-GO-PANI ternary nanocomposite has great potential application in removal of Pb(II) ions from industrial wastewater.

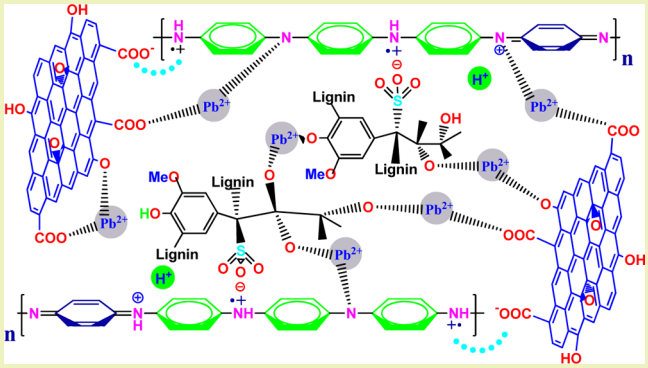

KEYWORDS: *Lignosulfonate, Graphene oxide, Polyaniline, Adsorption, Lead ions*

INTRODUCTION

Environmental contamination by industrial wastewater is a widespread problem, in particular the heavy metal ions. Heavy metal ions, such as lead ions, are highly toxic for animals and human beings.[1−4] Therefore, they should be removed from wastewater before discharge. Adsorption has been considered to be superior to other techniques to remove heavy metal ions due to its lower operating cost and convenience of design. Aiming at these contaminates of wastewater, many adsorbents were studied to solve the problem of waste aqueous soultions.[5−9]

As a typical conducting polymer, polyaniline (PANI) has been attracting great research interest in recent years because of its low cost, ease of preparation, and environmental stability. In addition, PANI contains a large amount of imine functional groups,[10−13] which can interact with some heavy metal ions from aqueous solutions.[14] On the basis of this characteristic, PANI and its derivatives and composites have been used for the adsorption of Cu(II),[13,15] Hg(II),[16,17] Co(II),[18] Ag(I),[19,20] Au(III)[21−23] Cr(VI),[11,13] Cd(II),[24] and Pb(II).[12,15]

Lignosulfonate (LS) has a large amounts of functional groups and a good performance of solubility in aqueous solution.[25] It has become increasingly valuable for its versatility in performance for chemicals such as resins, plastics, and fillers; and it has been widely applied in numerous industrial areas.[26] Furthermore, the functional groups on LS chains[27,28] make it potentially useful as an adsorbent material for removal of heavy metal ions from waste waters.[29−31]

Graphene, which is considered to be the basic building block of all graphitic forms (including carbon nanotube, graphite, and fullerence), is a single-atom thick two-dimensional carbon material.[32] It has been theorized to have a huge specific surface area,[33] leading to its potential applications in the environmental field as an effective adsorbent for pollutant elimination. Both sides of planar nanosheets of graphene are available for molecule adsorption, suggesting a high adsorption capacity. However, the use of graphene for down to earth applications like wastewater adsorption is limited. This mainly results from its difficulty in preparing composites with other materials because the surface of a graphene sheet has little reactive groups.[34] Graphene oxide (GO), a graphene precursor, can be easily modified with functional groups because it possesses many reactive groups including hydroxyl and epoxide groups and carboxyl and carbonyl groups.[35] Chemically derived graphene oxide obtained from graphite has revealed a variety of potential applications because of its easily functionalization and relatively cheap fabrication.[36,37]

The reactive groups on the surface of GO provide a good compatibility with polymers and form a GO/polymer composite with a stable structure, such as GO/PANI composite.[38−41] These nanocomposites have been studied because of their remarkable hydrophilicity, extraordinary nanostructure, and extensive potential application.[42−46] Con-

Received: January 14, 2014
Revised: March 11, 2014
Published: April 7, 2014

sidering the hydroxyl and epoxide groups located mostly on the surface of GO nanosheets, and the carboxyl and carbonyl groups decorated mainly at the edges of GO nanosheets, the adsorption presumably occurs on the surface of GO/polymer nanocomposites when GO/polymer nanomaterials were used as an adsorbent for removal of heavy metal ions from aqueous solutions.[47] Thus, an effective adsorbent with strong hydrophilicity, huge specific surface area, and a particular nanosheet structure could improve its adsorption capacity. Up to now, GO and its composites have been applied in the adsorption of heavy metal ions, such as Au(III),[48] Cu(II),[49] Cd(II),[47] and Pb(II) ions.[9,50,51]

In this work, a new adsorbent, lignosulfonate−graphene oxide−polyaniline ternary nanocomposite, was prepared by in situ polymerization of aniline and used for the removal of lead ions from aqueous solution. Synergistic effects of functional groups from lignosulfonate, polyaniline, and the high specific surface area of graphene oxide are expected to achieve a high performance for this new adsorbent for lead ions.

EXPERIMENTAL SECTION

Materials. Lignosulfonate (LS) was supplied by Shandong Longlive Biotechnology Co., Ltd. (Shandong, China) in powder form. Aniline was obtained from Sinopharm Chemical Reagent Co., Ltd. (Shanghai, China) and purified by distillation under reduced pressure prior to use. Ammonium persulfate (APS), expansible graphite, sulfuric acid (H_2SO_4), potassium permanganate ($KMnO_4$), hydrogen peroxide (H_2O_2), lead nitrate ($Pb(NO_3)_2$), and other solvents were purchased from Sinopharm Chemical Reagent Co., Ltd. (Shanghai, China) and used as without further treatment.

Preparation of Graphene Oxide. Graphene oxide (GO) was prepared from expansible graphite (100 mesh) using an airtight oxidation method.[52] Briefly, expansible graphite, $KMnO_4$, sulfuric acid (98%), a measuring cylinder and a Teflon reactor were completely cooled in a refrigerator at 0 °C before use. The Teflon reactor was placed in a stainless steel autoclave. The cooled expansible graphite (0.6 g) and $KMnO_4$ (3 g) were put into the reactor, and then sulfuric acid (30 mL) was added. As soon as the sulfuric acid was added, the reactor and stainless steel autoclave were covered and fastened down. The autoclave was kept at 0 °C for 2 h and then tightened up again; after that, it was heated at 110 °C in an oven for 2 h. The obtained mud was diluted with 500 mL of deionized water. With mechanical stirring, H_2O_2 (30%) was dripped into the suspension until the slurry turned golden yellow. The suspension was washed with 0.1 mol L^{-1} HCl and deionized water until its pH value reached 7 and humid GO was obtained. The product was dried in a 50 °C vacuum oven for 72 h to obtain GO powder.

Preparation of LS-GO-PANI Ternary Nanocomposite. The LS-GO-PANI ternary nanocomposite was prepared in a HCl aqueous solution with the LS and GO concentrations of 5 wt %. A typical polymerization of the nanocomposite was as follows. GO (0.104 g) was ultrasonically dissolved in an aqueous solution of hydrochloric acid (1.0 mol L^{-1}, 70 mL) in a 250 mL glass flask under ultrasonication (220 V, 200W) for 1 h, and then the suspension was kept in an ice bath for 0.5 h. Subsequently, LS (0.104 g) and aniline (1.83 mL, 20 mmol) was added to the GO suspension and stirred vigorously to form a mixture of LS-GO-aniline. APS (4.564 g, 20 mmol) was dissolved separately in an aqueous solution of hydrochloric acid (1.0 mol L^{-1}, 30 mL) to prepare an oxidant solution and was placed in an ice bath for 0.5 h. The APS solution was poured into the mixture of GO-LS-aniline and immediately stirred to ensure sufficient mixing before the polymerization began. Then, the polymerization was carried out in an ice bath for 24 h without stirring. The LS-GO-PANI ternary nanocomposite was isolated from the reaction mixture by filtration and washed with an excess amount of deionized water to remove the residual oxidant and other impurities. The product was dried at a 60 °C vacuum for 72 h. Herein, the pure PANI and GO-PANI nanocomposite with GO concentration of 10 wt % were prepared via the similar procedure above.

Lead Ions Adsorption. Adsorption tests of Pb(II) ions on the LS-GO-PANI ternary nanocomposite at varying adsorption time, initial pH value, adsorbent concentration, and initial Pb(II) ion concentration were carried out by a batch method. The desired pH value was adjusted using 0.1 mol L^{-1} HNO_3 or 0.1 mol L^{-1} $NaHCO_3$ solution. The Pb(II) ions stock solution was prepared by dissolving lead nitrate in deionized water. It was diluted with deionized water to a desired concentration. Typically, a test solution (25 mL) containing Pb(II) ions (200 mg L^{-1}) and dry LS-GO-PANI ternary nanocomposite (40 mg) were loaded in a 100 mL conical flask. The adsorption solution was stirred for 5 min, and then the adsorption proceeded under static conditions at 30 °C for 24 h to reach equilibrium. After a desired adsorption period, the nanocomposite was filtered from the solution, and then the concentration of Pb(II) ions in the filtrate after adsorption was measured by molar titration.[6]

The adsorbed amount of Pb(II) ions on the adsorbent was calculated according to the following eqs 1 and 2

$$Q = [(C_0 - C)V]/W \quad (1)$$

$$q = [(C_0 - C)/C_0] \times 100\% \quad (2)$$

where Q is the adsorption capacity (mg g^{-1}); C_0 and C are the lead ions' concentration before and after adsorption (mg L^{-1}), respectively; V is the initial volume of the lead ions solution (L); W is the weight of the added (g) ; and q is the adsorptivity (%).

Characterization. Morphological measurement of the LS-GO-PANI ternary nanocomposite was performed using field emission scanning electron microscopy (FE-SEM, FEI NanoSEM 230) and a transmission electron microscope (JEM-2010, Jeol). Elemental analysis of the LS-GO-PANI ternary nanocomposite was performed by an elemental analyzer (Vario EL cube). FTIR spectra were recorded on a Nicolet FTIR 5700 spectrophotometer in KBr pellets. UV−vis spectra were measured on a Varian Cary50 Conc spectrometer in the wavelength range of 200−1100 nm. A wide-angle X-ray diffraction scan was obtained using an Ultima III X-ray model diffractometer (Rigaku, Tokyo, Japan) with Cu Kα radiation at a scan rate of 10° min^{-1} in reflection mode.

Mathematical Models. The adsorption kinetic equations were fitted by pseudo-first-order (eq 3) and pseudo-second-order (eq 4) kinetic models.[4,53]

$$\ln(Q_e - Q_t) = \ln Q_e - k_1 t \quad (3)$$

$$t/Q_t = 1/(k_2 Q_e^{\,2}) + t/Q_e \quad (4)$$

where k_1 is the pseudo-first-order rate constant (h^{-1}), and k_2 is the pseudo-second-order kinetic rate constant (g mg^{-1} h^{-1}). Q_e and Q_t are the amounts of Pb(II) ions adsorbed per unit adsorbent (mg g^{-1}) at equilibrium and at time t (h), respectively.

The Langmuir and Freundlich isotherm models were used to describe and analyze adsorption equilibrium, as described by eqs 5 and 6.[4,53]

$$C_e/Q_e = C_e/Q_m + 1/(K_L Q_m) \quad (5)$$

$$\ln Q_e = \ln K_F + (1/n)\ln C_e \quad (6)$$

where Q_e is the amount of Pb(II) ions adsorbed (mg g^{-1}) at equilibrium, and C_e is the equilibrium concentration (mg L^{-1}). Q_m (mg g^{-1}) and K_L (L mg^{-1}) are the Langmuir constants related to the saturated adsorption capacity and adsorption energy, respectively. K_F [(mg g^{-1})(L $mg^{-1})^{1/n}$] and n are the Freundlich constants and indicate the adsorption capacity of the adsorbent and adsorption affinity for the adsorbate, respectively.

RESULTS AND DISCUSSION

Morphology. The typical FE-SEM images of the adsorbents and TEM image of the LS-GO-PANI ternary

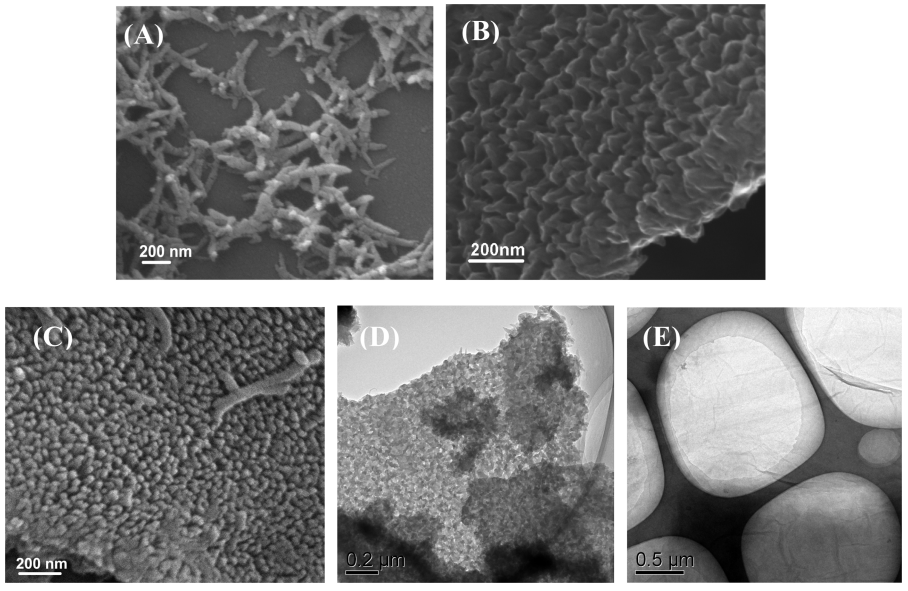

Figure 1. FE-SEM (A–C) and TEM (D,E) images of PANI (A), GO-PANI nanocomposite (B), LS-GO-PANI ternary nanocomposite (C,D), and GO (E).

Scheme 1. Illustration of Growth Mechanism of LS-GO-PANI Ternary Nanocomposite

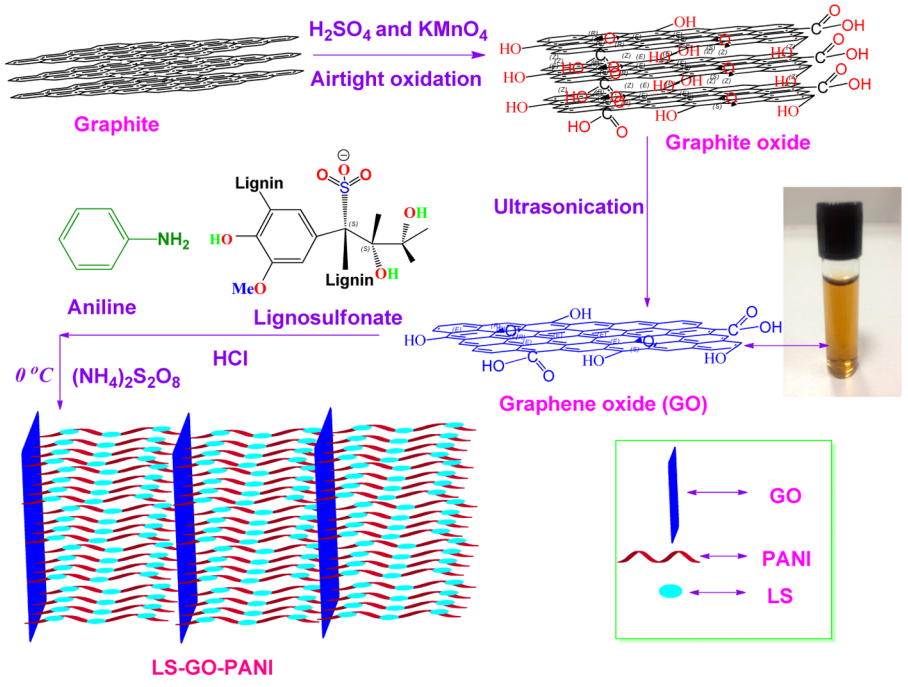

nanocomposite are shown in Figure 1. The FE-SEM image shows that PANI (Figure 1A) contains lots of nanofibers,[54,55] with the dimension of about 50 nm in diameter and 450–850 nm in length. From the TEM image of GO shown in Figure 1E, we can clearly see that the GO sample is almost transparent and exhibits a curly single layer with a smooth surface. As for the GO-PANI sample (Figure 1B), serated PANI arrays are evenly covered on GO nanosheets, indicating that the nucleation and growth processes of aniline monomers occurred on the surface of GO nanosheets. For the LS-GO-PANI ternary nanocomposite, the SEM and TEM images shown in Figure 1C and D clearly reveal that both surfaces of the GO nanosheets are homogeneously surrounded with nanofibers with an average diameter of 50 nm. It is clearly found that the LS-GO-PANI ternary nanocomposite has a larger special surface than the pure PANI. Thus, the LS-GO-PANI ternary nanocomposite can effectively faciliate the adsorptivity for the adsorbate.[37,56]

On the basis of the above experimental results, a formation mechanism of the LS-GO-PANI ternary nanocomposite is illustrated in Scheme 1. GO was produced from expansible graphite using an airtight oxidation method,[52] in which GO existed in a mixture of single and a few layer structures in solution. GO exhibits enormous active edges and oxygen-containing functional groups on its layers, providing compatibility with polymer matrices. These oxygen-containing functional groups on the GO surface make it easily dispersible in aqueous solution and may also act as nucleation sites for the PANI nanofibers attaching on its surfaces and edges.[41]

dx.doi.org/10.1021/sc500030v | ACS Sustainable Chem. Eng. 2014, 2, 1203–1211

Moreover, the $\pi-\pi$ stacking force in the special structure of GO was also in favor of the polymerization of aniline monomers occurring on the surface of GO nanosheets.[44,46] In a previous study,[42] it was reported that there were only heterogeneous nucleation in the *in situ* polymerization process of preparing a GO-PANI composite at a low polymerization temperature and low concentration of aniline; besides, a lower reactive temperature is also beneficial to form an ordered composite. Because the polymerization of aniline monomers in our study was carried out at a low polymerization temperature, the chemical oxidative polymerization process of the LS-GO-PANI ternary nanocomposite could be defined as three steps. First, the polymerization of aniline occurred at an aniline/aqueous interface when the APS solution was dropped into the LS-GO-aniline solution, and then initial polyaniline nanofibers formed via homogeneous nucleation at the initial stage of the polymerization.[57] Second, the LS chains were adsorbed on the surfaces of the initial polyaniline nanofibers because of the existence of electrostatic interactions between the polyaniline cations and the negatively charged sulfonic groups on the LS chains.[58] Third, the growth of these LS-PANI nanofibers proceeded on the surface of GO nanosheets by heterogeneous nucleation (as shown in Figure 1C). This is because the active sites on the GO surface would minimize the interfacial energy barrier between the solid surface and bulk solution,[42] which was beneficial to the growth of LS-PANI nanofibers on the solid substrates. Thus, the nanofibers would evenly grow on the surface of GO nanosheets and form long nanowire arrays at a low reaction temperature, and then the LS-GO-PANI ternary nanocomposite was achieved.

Structures the LS-GO-PANI Ternary Nanocomposite: Elemental Analysis. The elemental analysis shows that the LS-GO-PANI ternary nanocomposite has the following components: C, 61.00%; N, 10.41%; H, 5.49%; O, 9.38%; S, 4.09%; and Cl, 0.69%. The results reveals that the ternary nanocomposite contains three major components of LS, GO, and PANI. Moreover, the weight ratio of C and N in the nanocomposite (5.86) is higher than that of doped PANI (5.14)[42] because the GO and LS in the nanocomposite can increase the ratio.

FTIR Spectra. FTIR spectra of PANI, GO-PANI, and the LS-GO-PANI ternary nanocomposite are presented in Figure 2A. In the spectrum of PANI, the adsorption peaks at 1580 and

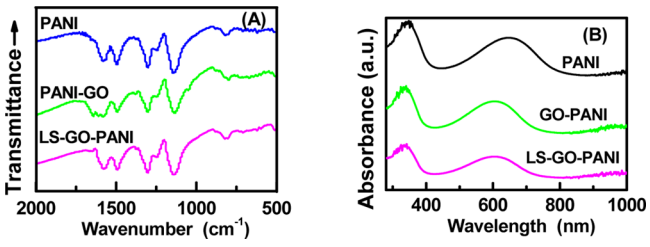

Figure 2. (A) FTIR and (B) UV−vis spectra of PANI, GO-PANI, and the LS-GO-PANI nanocomposite.

1645 cm^{-1} are assigned to the stretching of quinoid rings, and the peak at 1500 cm^{-1} is associated with the stretching of benzenoid rings.[12,28] Moreover, the band at 1140 cm^{-1} can be assigned to a vibration mode of the −NH− structure, and a peak at 1300 cm^{-1} should be due to the C−N stretching vibration in an alternative unit of quinoid−benzenoid−quinoid.[12,20] Two new peaks attributed to GO appeared in the spectrum of GO-PANI composite, i.e., the peaks at 1058 and 1635 cm^{-1}, which are associated with the vibration of C−O in alkoxy and −COOH functional groups.[41,59] However, compared with PANI and the GO-PANI composite, the spectrum of the LS-GO-PANI composite has a new peak at 1040 cm^{-1}. It should be attributed to S═O symmetric stretching of the $-SO_3$ groups on the LS chains.[28,60] These results signify that the as-prepared sample is a real nanocomposite of PANI, LS, and GO.

UV−vis Spectra. UV−vis spectra in Figure 2B show that there are two absorption bands of PANI at 348 and 644 nm with a free tail extended to the IR region. They could be assigned to a $\pi-\pi^*$ transition of the benzenoid ring and $n-\pi^*$ excitation of benzenoid to the quinoid ring in the polymer chain.[54] Furthermore, compared with PANI, the absorption bands of the two nanocomposites both show a little blue shift about 4 nm. The blue shift in the absorption bands of the GO-PANI nanocomposite can be due to the electronic interaction of carboxyl on the edges of GO nanosheets and the protonated PANI chain.[42] Besides, the hydrogen bonds between GO and the PANI backbone and $\pi-\pi$ stacking of GO nanosheets and PANI are also contributed to the blue shift.[43] Similarly, the blue shift of the LS-GO-PANI ternary nanocomposite is presumably due to the torsional twists of steric repulsion between the sulfonic and carboxylic groups and the hydrogens on the adjacent phenyl rings, which thus shortened the conjugation lengths.[28,41]

Adsorption of Pb(II) Ions. The adsorption capacities and adsorptivity of Pb(II) ions onto PANI, GO-PANI, and the LS-GO-PANI ternary nanocomposite are studied. It is found that the LS-GO-PANI ternary nanocomposite has the highest adsorption capacity and adsorptivity, which is up to 98.1 mg g^{-1} and 78.5%, respectively, whereas the adsorption capacities of PANI and GO-PANI are 95.7 and 85.7 mg g^{-1}, respectively. That is to say, the LS-GO-PANI ternary nanocomposite exhibits an enhanced adsorption capacity for Pb(II) ions than those of PANI and GO-PANI. This is attributed to the higher surface area of the LS-GO-PANI ternary nanocomposite[56,61] and the existence of a synergistic effect among the functional groups from PANI, LS, and GO in the LS-GO-PANI ternary nanocomposite. Therefore, the LS-GO-PANI ternary nanocomposite could be considered as a promising adsorbent for the removal of Pb(II) ions from aqueous solution.

Effect of Adsorption Time. The time allowed for adsorption between the adsorbate and adsorbent is an important factor for adsorption at equilibrium. Figure 3 shows the effect of adsorption time on the adsorption of

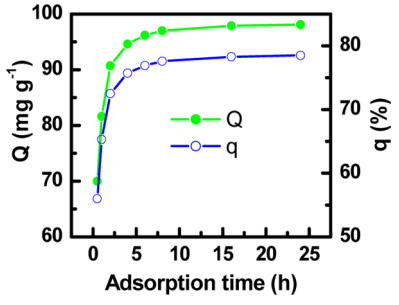

Figure 3. Effect of adsorption time on adsorption capacity (Q) and adsorptivity (q) of LS-GO-PANI at a Pb(II) ion concentration of 200 mg L^{-1} and the LS-GO-PANI concentration of 1.6 g L^{-1} with an initial pH value of 5.0 at 30 °C.

Pb(II) ions onto the LS-GO-PANI ternary nanocomposite. The adsorption capacity and adsorptivity go up rapidly at the beginning as the adsorption time increased. When the adsorption time is 2 h, the adsorptivity is 72.5%, and the adsorption capacity reaches 90.7 mg g^{-1}. It is shown that the adsorption capacity has reached 98.3% of the maximum in the first 4 h of the adsorption, indicating the adsorbent has an excellent property contrasted with other adsorbents.[7,10,12] The adsorption rate decreases gradually during the remaining adsorption time, which might be a result of the adsorption and desorption processes occurring after saturation of Pb(II) ions onto the LS-GO-PANI ternary nanocomposite surfaces.[62] However, the adsorption capacity and adsorptivity are almost constant at 98.1 mg g^{-1} and 78.5%, respectively, after 24 h, signifying that an equilibrium balance of adsorption is reached.

Effect of Initial pH Value. The effect of initial pH value is very significant for the adsorption of Pb(II) ions solution onto the LS-GO-PANI ternary nanocomposite (Figure 4) because

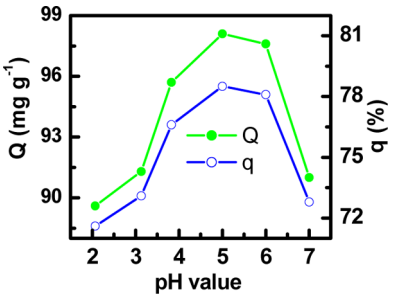

Figure 4. Effect of initial pH value on adsorption at a Pb(II) ions concentration of 200 mg L^{-1} and the LS-GO-PANI concentration of 1.6 g L^{-1} at 30 °C.

the adsorption of metal ions on solid particles is generally affected by pH values.[13] It is shown that the adsorption capacity of Pb(II) ions on the LS-GO-PANI ternary nanocomposite increases with increasing the pH value from 2.0 to 5.0. This is because high concentration of H^+ ions has a competitive adsorption with Pb(II) ions and influences the adsorption capacity of Pb(II) ions. When the initial pH value is 5.0, the adsorption capacity of Pb(II) ions reaches a maximum value of 98.1 mg g^{-1}. This phenomenon is attributed to the change in ionization state of the functional groups (carboxyl, hydroxyl, and amino groups) in the LS-GO-PANI ternary nanocomposite.[16] When the pH value is near or higher than 7.0, precipitations of $Pb(OH)_2$ occur, resulting in an inaccurate interpretation of adsorption. Typically, the initial pH value for the adsorption of Pb(II) ions is between 5.0 and 6.0.[7] This is also the application scope for the adsorption of Pb(II) ions from an industrial waste aqueous solution. Therefore, the next studies are performanced at a fixed pH value of 5.0.

Effect of Adsorbent Concentration. The effect of adsorbent concentration on adsorption of Pb(II) ions was studied with an initial Pb(II) ion concentration of 200 mg L^{-1} and the LS-GO-PANI concentration ranging from 0.4 to 3.2 g L^{-1} (Figure 5). Clearly, the adsorption capacity decreases with increasing adsorbent concentration, whereas the adsorptivity increases. The reason for this is that the surface per unit mass of the LS-GO-PANI ternary nanocomposite exposed to Pb(II) ions decreases when the amount of LS-GO-PANI decreases.[12] When the LS-GO-PANI ternary nanocomposite concentration is 0.4 g L^{-1}, the adsorption capacity is up to 158.1 mg g^{-1} and

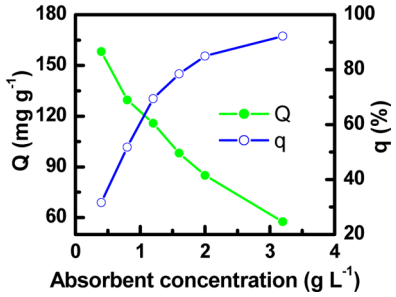

Figure 5. Effect of the LS-GO-PANI concentration on adsorption at a Pb(II) ions concentration of 200 mg L^{-1} at 30 °C.

the adsorptivity is 31.6%. However, the adsorption capacity is only 57.6 mg g^{-1} and the adsorptivity is 92.2% at the LS-GO-PANI ternary nanocomposite concentration of 3.2 g L^{-1}. Moreover, the adsorptivity increases slightly when the adsorbent concentration is higher than 1.6 g L^{-1}. Thus, the LS-GO-PANI ternary nanocomposite concentration of 1.6 g L^{-1} is deemed satisfactory on account of its adsorption capacity of 98.1 mg g^{-1} and adsorptivity of 78.5%. Because increasing the dosage of the LS-GO-PANI ternary nanocomposite is an invalid way for improving the adsorptivity, the following experiments are carried out at a constant adsorbent concentration of 1.6 g L^{-1}.

Effect of Initial Pb(II) Ions Concentration. The effect of variations in the initial Pb(II) ion concentration on the adsorption of the LS-GO-PANI ternary nanocomposite was studied (Figure 6). It is clearly observed that the adsorption

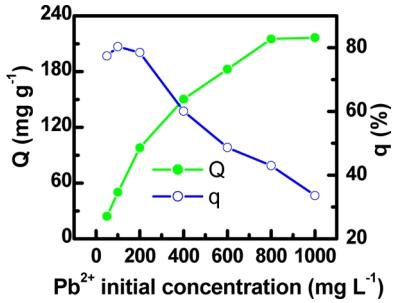

Figure 6. Effect of initial Pb(II) ions concentration on adsorption of the LS-GO-PANI ternary nanocomposite at 30 °C.

capacity increases as the initial Pb(II) ions concentration increases; however, the adsorptivity increases with the initial Pb(II) ions concentration below 100 mg g^{-1} and then decreases with increasing the concentration from 100 to 1000 mg g^{-1}. This is because with an increase in Pb(II) ions there is not enough of the LS-GO-PANI nanocomposite to adsorb Pb(II) ions. The adsorption attained saturatation; so, more Pb(II) ions cannot be adsorbed. Therefore, the adsorptivity decreased with an increase in Pb(II) ions concentration. When the initial Pb(II) ions concentration is 50 mg L^{-1}, the adsorption capacity and adsorptivity are 24.2 mg g^{-1} and 77.4%, respectively. In addition, when the initial Pb(II) ions concentration is 1000 mg L^{-1}, the adsorption capacity and adsorptivity are 216.4 mg g^{-1} and 33.6%, respectively, whereas the adsorption capacity and adsorptivity were 98.1 mg g^{-1} and 78.5% when the initial Pb(II) ions concentration was 200 mg L^{-1}. In order to achieve higher adsorptivity of Pb(II) ions, other studies in this work were carried out at the initial Pb(II) ions concentration of 200 mg L^{-1}. The maximum Pb(II) ion adsorption capacity of the

dx.doi.org/10.1021/sc500030v | ACS Sustainable Chem. Eng. 2014, 2, 1203−1211

LS-GO-PANI ternary nanocomposite compared with other related adsorbents[2−4,6,7,12,31,50] is listed in Table 1. Clearly, the LS-GO-PANI ternary nanocomposite demonstrated a high adsorption capacity of 216.4 mg g^{-1} for Pb(II) ions than other adsorbents.

Table 1. Adsorption Capacities of Other Related Adsorbents for Pb(II) Ions

adsorbent	conditions	Q (mg g^{-1})	ref
modified lignin from alkali glycerol	330 K, pH 6.0	9.0	2
porous carbon	298 K, pH 5.0	32.4	3
green algae	298 K, pH 5.0	140.84	4
sulfophenylenediamine copolymer	303 K, pH 5.0	161.6	6
graphene layer of carbonaceous	293 K, pH 5.6	30.05	7
polyaniline and multi-walled carbon nanotube	293 K, pH 5.0	22.2	12
lignin	293 K, pH 5.5	89.4	31
SiO_2/graphene composite	298 K, pH 6.0	113.6	50
LS-GO-PANI composite	303 K, pH 5.0	216.4	this work

Mathematical Models. Pseudo-first-order and pseudo-second-order kinetic models were used to investigate the process of Pb(II) ions adsorption on LS-GO-PANI. The pseudo-first-order model is mathematically equivalent to a mass action rate equation for adsorption kinetics, while the pseudo-second-order model assumes that the rate-limiting step is chemisorption of metal ions onto adsorbent binding sites.[4] The correlation coefficients of the pseudo-first-order and pseudo-second-order equations for the adsorption of Pb(II) ions onto LS-GO-PANI are listed in Table 2. Lines obtained of the plot

Table 2. Kinetic Parameters and Isothermal Models for Pb(II) Ions Adsorption on LS-GO-PANI Ternary Nanocomposite

parameter	value	parameter	value
pseudo-first-order model		pseudo-second-order model	
Q_e [mg g^{-1}]	16.84	Q_e [mg g^{-1}]	99.21
k_1 [h^{-1}]	0.2944	k_2 [g mg^{-1} h^{-1}]	50.52
R^2	0.9166	R^2	0.9999
Langmuir isotherm model		Freundlich isotherm model	
Q_m [mg g^{-1}]	250.0	K_F [(mg g^{-1}) (L $mg^{-1})^{1/n}$]	10.31
K_L [L mg^{-1}]	0.2944	$1/n$	0.5020
R^2	0.9945	R^2	0.9044

with linear regression coefficients (R^2) indicate the applicability of the pseudo-first-order and the pseudo-second-order models (Figure 7). Comparison of the correlation coefficients of the two equations for Pb(II) ions adsorption indicates that the pseudo-second-order kinetic model is more likely to predict the adsorption behavior over the whole range of adsorption. Thus, we can infer that the removal of Pb(II) ions by the LS-GO-PANI ternary nanocomposite is a process that is mainly controlled by the chemical interaction between Pb(II) ions and the binding sites.

In addition, the Langmuir and Freundlich sorption isotherm models were also used to investigate the adsorption of Pb(II) ions onto the LS-GO-PANI ternary nanocomposite (Table 2, Figure 8). The absorption data of LS-GO-PANI can be nicely fitted by the Langmuir absorption isotherm model with higher coefficients of 0.9916. The data failed to be fitted by the

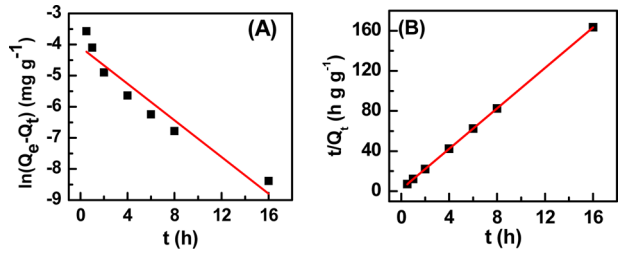

Figure 7. (A) Pseudo-first-order and (B) pseudo-second-order kinetic models of Pb(II) ions adsorption onto the LS-GO-PANI ternary nanocomposite.

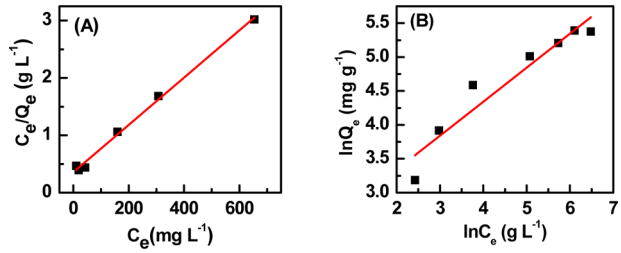

Figure 8. (A) Langmuir and (B) Freundlich isotherm models of Pb(II) ions adsorption onto the LS-GO-PANI ternary nanocomposite.

Freundlich model, although it is also widely used in adsorption studies. Langmuir's model of adsorption depends on the assumption that intermolecular forces decrease rapidly with distance and a structurally homogeneous adsorbent where all adsorption sites are identical and energetically equivalent and consequently predict the existence of monolayer coverage of the adsorbate at the outer surface of the adsorbent.[7] The isotherm equation further assumes that adsorption takes place at specific homogeneous sites within the adsorbent. It is then assumed that once a Pb(II) ion occupies a site no further adsorption can take place at that site. Therefore, the Langmuir model suggests that Pb(II) ions are absorbed by specific sites of LS-GO-PANI and form a monolayer.

Adsorption Mechanism. The reason for a high adsorption capacity of the Pb(II) ions onto LS-GO-PANI can be summarized as follows. First, the GO nanosheets have a huge specific surface area and large amounts functional groups such as carboxyl and lactone, which provide the nucleation sites for the growth of the PANI nanofibers and magnifiy the specific surface of the LS-GO-PANI ternary nanocomposite. Thus, the existence of GO on LS-GO-PANI increases the interaction areas between the adsorbent and the adsorbate in aqueous solution and can also effectively improve the adsorption capacity of Pb(II) ions. Also, the nanostructure of the LS-GO-PANI ternary nanocomposite works out the serious aggregation problem of PANI nanofibers, and it can facilitate interactions of the functional groups on the PANI nanofibers with Pb(II) ions.[42] Moreover, the strong interactions between functional groups of GO and PANI increased the steric hindrance effect of the nanocomposite.[63] However, the steric hindrance effect could stably bind the Pb(II) ions on the surface of LS-GO-PANI ternary nanocomposite, and it is also beneficial for improving the adsorptivity of Pb(II) ions. Second, as it is well known, PANI nanofibers carry large amounts of amine and imine functional groups simultaneously. The nitrogen of coexisting amine and imine functional groups is expected to have strong affinity to Pb(II) ions from an aqueous solution.[6] It is reasonable that the amine and imine functional

groups on the LS-GO-PANI ternary nanocomposite can form strong complexes with Pb(II) ions on LS-GO-PANI surfaces and thereby enhance the adsorption capacity of Pb(II) ions on LS-GO-PANI, as described in Scheme 2. Similarly, the LS

Scheme 2. Possible Adsorption Mechanism of Pb(II) Ions on LS-GO-PANI Ternary Nanocomposite

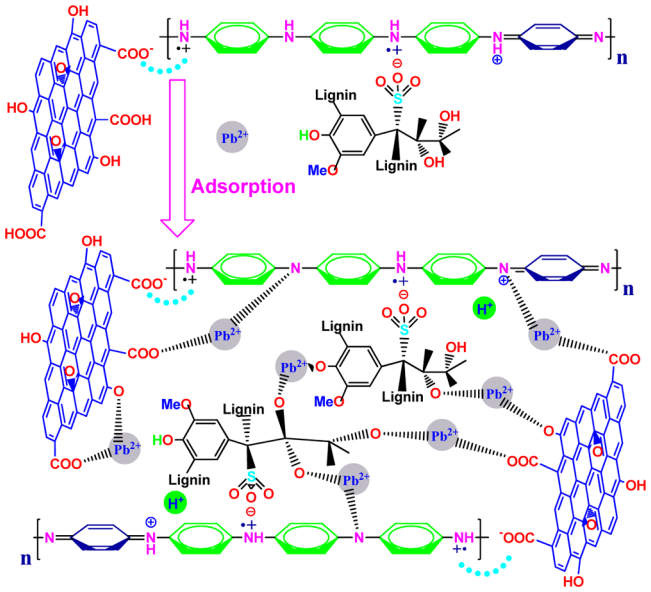

chains possess abundant electronegative sulfonic groups,[28] whereas the Pb(II) ions are electropositive. The adsorption results suggested that electrostatic interactions between the Pb(II) cations and sulfonic anions on the LS chain could be also operative for the Pb(II) ions adsorption on LS-GO-PANI. Besides, there are abundant carboxyl and phenolic units on LS chains, which could form bidentate complexes with Pb(II) ions in the aqueous solution when the value of adsorption pH was higher than 4.[31]

Third, the synergistic effect of the function groups on these three components certainly plays a key role in the adsorption. The amino groups in PANI units may improve the coordinate ability of sulfonic groups on LS chains and carboxyl groups on GO nanosheets for Pb(II) ions. Owing to the undesirable distance determined by the conformation, the carboxyl groups and sulfonic groups in two neighboring molecular chains are unable to together coordinate the Pb(II) ions. However, the amino groups on PANI chains afford another site for the coordinate of Pb(II) ions. Hence, the LS-GO-PANI ternary nanocomposite can vigorously bind the Pb(II) ions in the synergistic effect of the functional groups.

CONCLUSIONS

A new adsorbent, LS-GO-PANI ternary nanocomposite, has been successfully prepared by using an *in situ* polymerization of aniline with the existence of lignosulfonate and graphene oxide in a hydrochloric acid aqueous solution. The nanocomposite exhibits excellent adsorption characteristics for Pb(II) ions. The functional groups and high specific surface area of the LS-GO-PANI ternary nanocomposite enhance its adsorption ability of Pb(II) ions. The maximum adsorption capacity for Pb(II) ions is up to 216.4 mg g^{-1}. The adsorption kinetics and isotherms studies reveal that the adsorption process of Pb(II) followed the pseudo-second-order kinetic and Langmuir isotherm models. This indicates that the removal of Pb(II) ions by the LS-GO-PANI ternary nanocomposite is a process mainly controlled by the chemical interaction between adsorbate and binding sites. Moreover, the LS-GO-PANI ternary nanocomposite exhibits a higher adsorption capacity than those of PANI and GO-PANI, suggesting the existence of a synergistic effect of the functional groups on the LS-GO-PANI ternary nanocomposite. The results demonstrate that the LS-GO-PANI ternary nanocomposite can be utilized as an effective and economical adsorbent for the removal of Pb(II) ions from industrial wastewater.

AUTHOR INFORMATION

Corresponding Author

*E-mail: qiufenglv@163.com, qiufenglvfzu@gmail.com.

Notes

The authors declare no competing financial interest.

ACKNOWLEDGMENTS

This work was supported by the Natural Science Foundation of Fujian Province, China (2012J01201), and the Science-Technology Foundation of Education Bureau of Fujian Province, China (JA12031).

REFERENCES

(1) Cao, C. Y.; Qu, J.; Wei, F.; Liu, H.; Song, W. G. Superb adsorption capacity and mechanism of flowerlike magnesium oxide nanostructures for lead and cadmium ions. *ACS Appl. Mater. Interfaces* **2012**, *4*, 4283−4287.

(2) Demirbas, A. Adsorption of lead and cadmium ions in aqueous solutions onto modified lignin from alkali glycerol delignication. *J. Hazard. Mater.* **2004**, *109*, 221−226.

(3) Saleh, T. A.; Gupta, V. K.; Al-Saadi, A. A. Adsorption of lead ions from aqueous solution using porous carbon derived from rubber tires: Experimental and computational study. *J. Colloid Interface Sci.* **2013**, *396*, 264−269.

(4) Gupta, V. K.; Rastogi, A. Biosorption of lead from aqueous solutions by green algae *Spirogyra* species: Kinetics and equilibrium studies. *J. Hazard. Mater.* **2008**, *152*, 407−414.

(5) Cheng, C.; Wang, J. N.; Yang, X.; Li, A.; Philippe, C. Adsorption of Ni(II) and Cd(II) from water by novel chelating sponge and the effect of alkali-earth metal ions on the adsorption. *J. Hazard. Mater.* **2014**, *264*, 332−341.

(6) Lü, Q. F.; Huang, M. R.; Li, X. G. Synthesis and heavy-metal-ion sorption of pure sulfophenylenediamine copolymer nanoparticles with intrinsic conductivity and stability. *Chem.—Eur. J.* **2007**, *13*, 6009−6018.

(7) Machida, M.; Mochimaru, T.; Tatsumoto, H. Lead(II) adsorption onto the graphene layer of carbonaceous materials in aqueous solution. *Carbon* **2006**, *44*, 2681−2688.

(8) Sun, L.; Yu, H.; Fugetsu, B. Graphene oxide adsorption enhanced by in situ reduction with sodium hydrosulfite to remove acridine orange from aqueous solution. *J. Hazard. Mater.* **2012**, *203*−*204*, 101−110.

(9) Yang, Y. F.; Xie, Y. L.; Pang, L. C.; Li, M.; Song, X. H.; Wen, J. G.; Zhao, H. Y. Preparation of reduced graphene oxide/poly(acrylamide) nanocomposite and its adsorption of Pb(II) and methylene blue. *Langmuir* **2013**, *29*, 10727−10736.

(10) Li, X. G.; Feng, H.; Huang, M. R. Strong adsorbability of mercury ions on aniline/sulfoanisidine copolymer nanosorbents. *Chem—Eur. J.* **2009**, *15*, 4573−4581.

(11) Guo, X.; Fei, G. T.; Su, H.; De Zhang, L. High-performance and reproducible polyaniline nanowire/tubes for removal of Cr(VI) in aqueous solution. *J. Phys. Chem. C* **2011**, *115*, 1608−1613.

(12) Shao, D.; Chen, C.; Wang, X. Application of polyaniline and multiwalled carbon nanotube magnetic composites for removal of Pb(II). *Chem. Eng. J.* **2012**, *185−186*, 144−150.
(13) Kong, Y.; Wei, J.; Wang, Z.; Sun, T.; Yao, C.; Chen, Z. Heavy metals removal from solution by polyaniline/palygorskite composite. *J. Appl. Polym. Sci.* **2011**, *122*, 2054−2059.
(14) Gordana, C. M. Recent advances in polyaniline composites with metals, metalloids and nonmetals. *Synth. Met.* **2013**, *170*, 31−56.
(15) Jiang, N.; Xu, Y.; Dai, Y.; Luo, W.; Dai, L. Polyaniline nanofibers assembled on alginate microsphere for Cu^{2+} and Pb^{2+} uptake. *J. Hazard. Mater.* **2012**, *215*, 17−24.
(16) Cui, H.; Qian, Y.; Li, Q.; Zhang, Q.; Zhai, J. Adsorption of aqueous Hg (II) by a polyaniline/attapulgite composite. *Chem. Eng. J.* **2012**, *211−212*, 216−223.
(17) Wang, J.; Deng, B.; Chen, H.; Wang, X.; Zheng, J. Removal of aqueous Hg (II) by polyaniline: Sorption characteristics and mechanisms. *Environ. Sci. Technol.* **2009**, *43*, 5223−5228.
(18) Silva, R.; Asefa, T. Noble metal-free oxidative electrocatalysts: polyaniline and Co(II)-polyaniline nanostructures hosted in nanoporous silica. *Adv. Mater.* **2012**, *24*, 1878−1883.
(19) He, Z. W.; Lü, Q. F.; Zhang, J. Y. Facile preparation of hierarchical polyaniline-lignin composite with a reactive silver-ion adsorbability. *ACS Appl. Mater. Interfaces* **2012**, *4*, 369−374.
(20) Lü, Q.-F.; Luo, J.-J.; Lin, T.-T.; Zhang, Y.-Z. Novel lignin−poly(*N*-methylaniline) composite sorbent for silver ion removal and recovery. *ACS Sustainable Chem. Eng.* **2014**, *2*, 465−471.
(21) Lee, Y.; Chang, C.; Yau, S.; Fan, L.; Yang, Y.; Yang, L. O.; Itaya, K. Conformations of polyaniline molecules adsorbed on Au(111) probed by in situ STM and ex Situ XPS and NEXAFS. *J. Am. Chem. Soc.* **2009**, *131*, 6468−6474.
(22) Fan, X.; Liu, L.; Guo, Z.; Gu, N.; Xu, L.; Zhang, Y. Facile synthesis of networked gold nanowires based on the redox characters of aniline. *Mater. Lett.* **2010**, *64*, 2652−2654.
(23) He, Z. W.; He, L. H.; Yang, J.; Lü, Q. F. Removal and recovery of Au(III) from aqueous solution using a low-cost lignin-based biosorbent. *Ind. Eng. Chem. Res.* **2013**, *52*, 4103−4108.
(24) Mansour, M. S.; Ossman, M. E.; Farag, H. A. Removal of Cd (II) ion from waste water by adsorption onto polyaniline coated on sawdust. *Desalination* **2011**, *272*, 301−305.
(25) Janaki, V.; Oh, B. T.; Shanthi, K.; Lee, K. J.; Ramasamy, A.; Kamala, K. S. Polyaniline/chitosan composite: an eco-friendly polymer for enhanced removal of dyes from aqueous solution. *Synth. Met.* **2012**, *162*, 974−980.
(26) He, Z.-W.; Yang, J.; Lü, Q.-F.; Lin, Q. Effect of structure on the electrochemical performance of nitrogen- and oxygen-containing carbon micro/nanospheres prepared from lignin-based composites. *ACS Sustainable Chem. Eng.* **2013**, *1*, 334−340.
(27) Gupta, G.; Birbilis, N.; Cook, A. B.; Khanna, A. S. Polyaniline−lignosulfonate/epoxy coating for corrosion protection of AA2024-T3. *Corros. Sci.* **2013**, *67*, 256−267.
(28) Lü, Q. F.; Wang, C. Y.; Cheng, X. S. One-step preparation of conductive polyaniline-lignosulfonate composite hollow nanospheres. *Microchim. Acta* **2010**, *169*, 233−239.
(29) Parajuli, D.; Inoue, K.; Ohto, K.; Oshima, T.; Murota, A.; Funaoka, M.; Makino, K. Adsorption of heavy metals on crosslinked lignocatechol: a modified lignin. *React. Funct. Polym.* **2005**, *62*, 129−139.
(30) Lü, Q. F.; Zhang, J. Y.; He, Z. W. Controlled preparation and reactive silver-ion sorption of electrically conductive poly(N-butylaniline)-lignosulfonate composite nanospheres. *Chem−Eur. J.* **2012**, *18*, 16571−16579.
(31) Guo, X.; Zhang, S.; Shan, X. Q. Adsorption of metal ions on lignin. *J. Hazard. Mater.* **2008**, *151*, 134−142.
(32) Novoselov, K. S.; Geim, A. K.; Morozov, S. V.; Jiang, D.; Zhang, Y.; Dubonos, S. V.; Grigorieva, I. V.; Firsov, A. A. Electric field effect in atomically thin carbon films. *Science* **2004**, *306*, 666−669.
(33) Geim, A. K.; Novoselov, K. S. The rise of graphene. *Nat. Mater.* **2007**, *6*, 183−191.
(34) Stankovich, S.; Dikin, D. A.; Dommett, G. H. B.; Kohlhaas, K. M.; Zimney, E. J.; Stach, E. A.; Piner, R. D.; Nguyen, S. T.; Ruoff, R. S. Graphene-based composite materials. *Nature* **2006**, *442*, 282−286.
(35) Dikin, D. A.; Stankovich, S.; Zimney, E. J.; Piner, R. D.; Dommett, G. H.; Evmenenko, G.; Nguyen, S. T.; Ruoff, R. S. Preparation and characterization of graphene oxide paper. *Nature* **2007**, *448*, 457−460.
(36) Cheng, C.; Deng, J.; Lei, B.; He, A.; Zhang, X.; Ma, L.; Li, S.; Zhao, C. S. Toward 3D graphene oxide gels based adsorbents for high-efficient water treatment via the promotion of biopolymers. *J. Hazard. Mater.* **2013**, *263*, 467−478.
(37) Bradder, P.; Ling, S. K.; Wang, S.; Liu, S. Dye adsorption on layered graphite oxide. *J. Chem. Eng. Data* **2011**, *56*, 138−141.
(38) Huang, Y. F.; Lin, C. W. Polyaniline-intercalated graphene oxide sheet and its transition to a nanotube through a self-curling process. *Polymer* **2012**, *53*, 1079−1085.
(39) Chen, G. L.; Shau, S. M.; Juang, T. Y.; Lee, R. H.; Chen, C. P.; Suen, S. Y.; Jeng, R. J. Single-layered graphene oxide nanosheet/polyaniline hybrids fabricated through direct molecular exfoliation. *Langmuir* **2011**, *27*, 14563−14569.
(40) Yan, X.; Chen, J.; Yang, J.; Xue, Q.; Miele, P. Fabrication of free-standing, electrochemically active, and biocompatible graphene oxide-polyaniline and graphene-polyaniline hybrid papers. *ACS Appl. Mater. Interfaces* **2010**, *2*, 2521−2529.
(41) Huang, Y. F.; Lin, C. W. Facile synthesis and morphology control of graphene oxide/polyaniline nanocomposites via in-situ polymerization process. *Polymer.* **2012**, *53*, 2574−2582.
(42) Xu, J.; Wang, K.; Zu, S. Z.; Han, B. H.; Wei, Z. Hierarchical nanocomposites of polyaniline nanowire arrays on graphene oxide sheets with synergistic effect for energy storage. *ACS Nano* **2010**, *4*, 5019−5026.
(43) Wang, H. L.; Hao, Q. L.; Yang, X. J.; Lu, L. D.; Wang, X. Effect of graphene oxide on the properties of its composite with polyaniline. *ACS Appl. Mater. Interfaces* **2010**, *2*, 821−828.
(44) Zhu, J.; Chen, M.; Qu, H.; Zhang, X.; Wei, H.; Luo, Z.; Colorado, H. A.; Wei, S.; Guo, Z. Interfacial polymerized polyaniline/graphite oxide nanocomposites toward electrochemical energy storage. *Polymer.* **2012**, *53*, 5953−5964.
(45) Liu, Y.; Deng, R.; Wang, Z.; Liu, H. Carboxyl-functionalized graphene oxide−polyaniline composite as a promising supercapacitor material. *J. Mater. Chem.* **2012**, *22*, 13619−13624.
(46) Zhang, W. L.; Park, B. J.; Choi, H. J. Colloidal graphene oxide/polyaniline nanocomposite and its electrorheology. *Chem. Commun.* **2010**, *46*, 5596−5598.
(47) Deng, X.; Lü, L.; Li, H.; Luo, F. The adsorption properties of Pb(II) and Cd(II) on functionalized graphene prepared by electrolysis method. *J. Hazard. Mater.* **2010**, *183*, 923−930.
(48) Liu, L.; Li, C.; Bao, C.; Jia, Q.; Xiao, P.; Liu, X.; Zhang, Q. Preparation and characterization of chitosan/graphene oxide composites for the adsorption of Au(III) and Pd(II). *Talanta* **2012**, *93*, 350−357.
(49) Yang, S. T.; Chang, Y.; Wang, H.; Liu, G.; Chen, S.; Wang, Y.; Liu, Y.; Cao, A. Folding/aggregation of graphene oxide and its application in Cu^{2+} removal. *J. Colloid Interface Sci.* **2010**, *351*, 122−127.
(50) Hao, L.; Song, H.; Zhang, L.; Wan, X.; Tang, Y.; Lv, Y. SiO_2/graphene composite for highly selective adsorption of Pb(II) ion. *J. Colloid Interface Sci.* **2012**, *369*, 381−387.
(51) Yang, X.; Chen, C. L.; Li, J. X.; Zhao, G. X.; Ren, X. M.; Wang, X. K. Graphene oxide-iron oxide and reduced graphene oxide-iron oxide hybrid materials for the removal of organic and inorganic pollutants. *RSC Adv.* **2012**, *2*, 8821−8826.
(52) Bao, C.; Song, L.; Xing, W.; Yuan, B.; Wilkie, C. A.; Huang, J.; Guo, Y.; Hu, Y. Preparation of graphene by pressurized oxidation and multiplex reduction and its polymer nanocomposites by masterbatch-based melt blending. *J. Mater. Chem.* **2012**, *22*, 6088−6096.
(53) Senthilkumaar, S.; Varadarajan, P. R.; Porkodi, K.; Subbhuraam, C. V. Adsorption of methylene blue onto jute fiber carbon: Kinetics and equilibrium studies. *J. Colloid Interface Sci.* **2005**, *84*, 78−82.

(54) Chen, J.; Chao, D.; Lu, X.; Zhang, W. Novel interfacial polymerization for radially oriented polyaniline nanofibers. *Mater. Lett.* **2007**, *61*, 1419−1423.
(55) Chiou, N.-R.; Lu, C.; Guan, J.; Lee, L. J.; Epstein, A. J. Growth and alignment of polyaniline nanofibres with superhydrophobic, superhydrophilic and other properties. *Nat. Nanotechnol.* **2007**, *2*, 354−357.
(56) Ayad, M. M.; El-Nasr, A. A. Adsorption of cationic dye (methylene blue) from water using polyaniline nanotubes. *J. Phys. Chem. C* **2010**, *114*, 14377−14383.
(57) Li, D.; Kaner, R. B. Shape and aggregation control of nanoparticles: not shaken, not stirred. *J. Am. Chem. Soc.* **2006**, *128*, 968−975.
(58) Ouyang, X.; Deng, Y.; Qian, Y.; Zhang, P.; Qiu, X. Adsorption characteristics of lignosulfonates in salt-free and salt-added aqueous solutions. *Biomacromolecules* **2011**, *12*, 3313−3320.
(59) Chen, G. L.; Shau, S. M.; Juang, T. Y.; Lee, R. H.; Chen, C. P.; Suen, S. Y.; Jeng, R. J. Single-layered graphene oxide nanosheet/polyaniline hybrids fabricated through direct molecular exfoliation. *Langmuir* **2011**, *27*, 14563−14569.
(60) Lü, Q. F.; Zhang, J. Y.; Yang, J.; He, Z. W.; Fang, C. Q.; Lin, Q. L. Self-assembled poly(*N*-methylaniline)−lignosulfonate spheres: From silver-ion adsorbent to antimicrobial material. *Chem.—Eur. J.* **2013**, *19*, 10935−10944.
(61) Ramesha, G. K.; Vijaya Kumara, A.; Muralidhara, H. B.; Sampath, S. Graphene and graphene oxide as effective adsorbents toward anionic and cationic dyes. *J. Colloid Interface Sci.* **2011**, *361*, 270−277.
(62) Ai, L. H.; Zhang, C. Y.; Chen, Z. L. Removal of methylene blue from aqueous solution by a solvothermal-synthesized graphene/magnetite composite. *J. Hazard. Mater.* **2011**, *192*, 1515−1524.
(63) Wu, Y.; Phillips, J. A.; Liu, H.; Yang, R.; Tan, W. Carbon nanotubes protect DNA strands during cellular delivery. *ACS Nano* **2008**, *2*, 2023−2028.